



Impact of Ag-Doped on the Ferromagnetic-Metallic Transition in $\text{Pr}_{0.75}\text{Na}_{0.25}\text{MnO}_3$ Manganites

N Khairulzaman¹, N Ibrahim², S Shamsuddin^{3*}

^{1,3}Ceramics and Amorphous Group, Faculty of Applied Sciences and Technology, Pagoh Higher Education Hub, Universiti Tun Hussein Onn Malaysia, 84600 Pagoh, Johor, Malaysia

²Faculty of Applied Sciences, Universiti Teknologi MARA, 40450 Shah Alam, Selangor, Malaysia.

*Corresponding author E-mail: suhadir@uthm.edu.my

Abstract

Monovalent doped $\text{Pr}_{0.75}\text{Na}_{0.25-y}\text{Ag}_y\text{MnO}_3$ ($y = 0-0.10$) manganite have been investigated using X-ray diffraction (XRD) and scanning electron microscope (SEM) as well as DC electrical resistivity and AC susceptibility measurement to clarify the influence of Ag-doped on charge ordering (CO) state. XRD analysis revealed all samples consists of essentially single phase and crystallized in an orthorhombic structure with space group $Pnma$. SEM images of $\text{Pr}_{0.75}\text{Na}_{0.25-y}\text{Ag}_y\text{MnO}_3$ compound shows the successful substitution of Ag^+ ions with the enhancement of the grains boundaries and sizes as well as the compaction of particles. On the other hand, resistivity and susceptibility measurements showed that the $y = 0$ sample exhibits insulating behavior and anti-ferromagnetic. Interestingly, the ferromagnetic-metallic transition was observed for $y = 0.05$ due to the revival of double-exchange (DE) mechanism as a result of weakening the Jahn-Teller effect which caused the CO state to be weakened. However, increasing of Ag-doped up to $y = 0.10$ induce back its transition into anti-ferromagnetic insulating behavior suggestively due to the weakening of DE mechanism.

Keywords: Charge Ordered; Double Exchange Mechanis; Electrical Transport Properties; Magnetic Properties; X-Ray Diffraction.

1. Introduction

This Hole-doped perovskite manganites with the general formula $\text{Re}_{1-x}\text{A}_x\text{MnO}_3$ where Re is trivalent rare-earth ion (Pr^{3+} , La^{3+} , Nd^{3+} , Dy^{3+}) and A is divalent (Ca^{2+} , Sr^{2+} , Cr^{2+}) or monovalent (Ag^+ , K^+ , Na^+) alkaline earth ions have received remarkable attention since discovery the Colossal Magnetoresistance (CMR) effect due to their unique magnetic and transport properties as well as the potential application at low temperature [1,2]. Commonly, these behaviors can be associated with the double exchange (DE) interaction involving the exchange of Mn^{3+} with Mn^{4+} which favor the ferromagnetic metallic (FMM) state [3] and Jahn Teller interaction that dominated the Mn^{3+} ion causing the behavior of paramagnetic insulating (PMI) [4] as well as charge ordering (CO) state. Generally, the CO can be linked to the localization of the charge and then restrict the electron to hop from one site to another site causing the manganite to exhibit an insulating or semiconducting behavior [5, 6]. Among the CO systems, the $\text{Pr}_{0.75}\text{Na}_{0.25}\text{MnO}_3$ has attracted interest due to the existence of CO transition at a higher temperature compared to antiferromagnetic (AFM) ordering ($T_{\text{CO}} \sim 260$ K, $T_{\text{N}} \sim 160$ K) [7,8].

Quite recently, several reports suggest the element substitution at A-site of monovalent doped manganites were modified their average ionic radius of A-site cation $\langle r_{\text{A}} \rangle$ and simultaneously affected the magnetic and electrical transport properties of compound [9,10]. For example, substitutions of K^+ ions at A-site of $\text{Pr}_{0.75}\text{Na}_{0.25-x}\text{K}_x\text{MnO}_3$ shows the interesting phenomena where the increment of K^+ ions suppress the CO state as well as induce the ferromagnetic-metallic transition at lower temperature with increasing of T_{C} and T_{MI} due to the reduction in MnO_6 octahedral distortion consequently enhanced double exchange (DE)

mechanism. [11]. Furthermore, the substitution of Ag ions on the $\text{Pr}_{0.5}\text{Sr}_{0.5-x}\text{Ag}_x\text{MnO}_3$ was inducing the antiferromagnetic into ferromagnetic follow by a paramagnetic transition at the lower temperature due to the variation of both mean radius of A-site and rate of $\text{Mn}^{3+}/\text{Mn}^{4+}$ with the increment of Ag concentration. [12]

On the other hand, scanning electron microscope (SEM) measurement have been useful in providing valuable information on the surface morphology of the compound including manganites, which can help to give a better understanding, especially on the morphological study [13, 11]. For instance, the substitution of Cr^{3+} and Co^{3+} at Mn site of the $\text{Pr}_{0.75}\text{Na}_{0.25}\text{MnO}_3$ were changed the surface morphology of the samples especially on the grain boundary and grain size as well as the porosity of the samples due to the difference of ionic radius [14, 15]. Thus, considering all of the above, studies on $\text{Pr}_{0.75}\text{Na}_{0.25-y}\text{Ag}_y\text{MnO}_3$ is expected to provide information about CO states as well as deliver new information on the morphological study. However, to our knowledge, the $\text{Pr}_{0.75}\text{Na}_{0.25-y}\text{Ag}_y\text{MnO}_3$ system has not been previously reported.

On this study, the transition element of silver with single ion was substituted at the A-site of the $\text{Pr}_{0.75}\text{Na}_{0.25-y}\text{Ag}_y\text{MnO}_3$ in order to investigate its effect on the structure and surface morphology as well as electrical and magnetic properties. In addition, values of density and porosity are also presented and discussed.

2. Experiment Methods

The $\text{Pr}_{0.75}\text{Na}_{0.25-y}\text{Ag}_y\text{MnO}_3$ ($y = 0, 0.05$ and 0.10) manganite samples were synthesized using the conventional solid-state reaction method. The powders with high purity ($\geq 99.99\%$) of

Table 1. MI transition temperature (T_{MI}), Curie temperature (T_C), Neel temperature (T_N), lattice parameters, unit cell volume (V), density (D) and porosity (C) of $\text{Pr}_{0.75}\text{Na}_{0.25-y}\text{Ag}_y\text{MnO}_3$ ($0 \leq y \leq 0.10$)

Samples	T_{MI} (K) ± 0.1	T_C (K) ± 0.1	T_N (K) ± 0.1	Lattice parameter ± 0.001			$V(\text{\AA})$ ± 0.1	$D(\text{g/cm}^3)$ ± 0.01	C (%) ± 0.01
				a (\AA)	b (\AA)	c (\AA)			
$y = 0.0$	-	-	125.0	5.432	7.680	5.451	227.4	6.26	6.31
$y = 0.05$	110.0	123.0	-	5.437	7.697	5.452	228.1	6.41	3.68
$y = 0.10$	-	-	126.0	5.459	7.705	5.455	229.5	6.54	1.01

Pr_2O_3 , Na_2CO_3 , Ag_2O and MnO_2 were carefully mixed and ground in appropriate stoichiometric ratio follow with calcination process at a temperature of 1000°C for 24 hours with one intermediate grinding. The calcinated powders were pressed under 5 tones into pellet form with a 13 mm diameter and 2–3 mm thickness. Finally, the pellets forms were sintered at 1200°C for 24 hours in air. The samples were examined using powder X-ray diffraction (XRD) Bruker D8 Advance model with Cu $K\alpha$ radiation (1.5440 \AA) at room temperature in order to determine the structure. The surface morphology of the samples was observed using Hitachi SU1310 scanning electron microscope (SEM) with magnification 5kX. The AC susceptibility (χ') of the samples were carried out using an AC susceptometer system manufactured by CryoBIND-T system in conjunction with its real component resolved using a 7265 DSP lock-in amplifier. The temperature dependent resistivity (ρ) were carried out under zero magnetic field using the standard four point-probe technique contact with silver point where the sample was placed on the head of a closed cycle refrigerator device Model CTI Cryogenics at low temperature in a range of 50–300 K. The values of porosity, C were determined using the following formula

$$C = 1 - \frac{D}{D_x}$$

where D is the bulk density using Archimedes principle and D_x is the x-ray densities calculated from the lattice parameters.

3. Results and Discussions

Figure 1 shows the powder X-ray diffraction (XRD) pattern for $\text{Pr}_{0.75}\text{Na}_{0.25-y}\text{Ag}_y\text{MnO}_3$ ($y = 0-0.10$) manganites. XRD analysis revealed all samples were in single phase and the crystal structure was indexed as an orthorhombic perovskite-structured whose unit cell belongs to the space group $Pnma$ reliable with the previous study that reported the structure [16, 17]. The result from XRD was analyzed using X'Pert HighScore programme in order to confirm the crystalline phase of the compound. Table 1 shows the values of metal insulator (MI), transition temperature (T_{MI}), Curie temperature (T_C) Neel temperature (T_N), lattices parameter, unit cell volume (V), density (D) and porosity (C) for all samples. It was found that the lattice parameter of all samples continuously increased with Ag content indicate successful substitution of Ag^+ in the crystal lattice suggestively due to the difference of ionic radius [16,18]. Ag^+ ions with larger ionic radius ($r_{\text{Ag}^+} = 1.280 \text{ \AA}$) was suggested to substitute Na^+ ions with smaller ionic radius ($r_{\text{Na}^+} = 1.240 \text{ \AA}$). In the present study, the increasing in values of density (D), as well as decrease in porosity with Ag content, shows a good agreement with the changing of unit cell volume (V) indicating a successful substitution of Ag^+ ions in the system.

The effect of Ag-doped on the surface morphology with the composition of $y = 0-0.10$ samples was shown as in Figure 2. The microstructure and morphology of all samples were analysed using a scanning electron microscope (SEM) with 5kX magnification. For $y = 0$ sample, the grain was found an irregular shape compared to $y = 0.05$ and 0.10 samples while the grain boundaries showed an improvement as the Ag content increase indicated suggestively successful substitution of Ag^+ ions in the compound as a result of a difference in ionic radius between Na^+ and Ag^+ ions. A similar suggestion was also proposed for $\text{Pr}_{0.75}\text{Na}_{0.25}\text{Mn}_{1-x}\text{Cr}_x\text{O}_3$ by [14]. In the presence of study, the

improvement of connectivity between grains was also clearly seen with increasing of Ag doping.

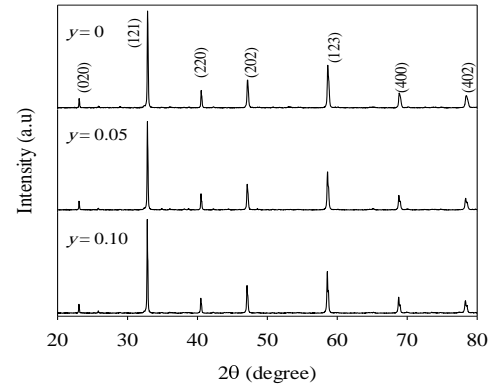
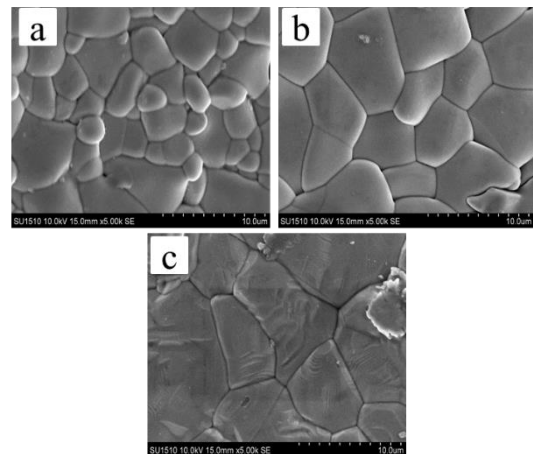
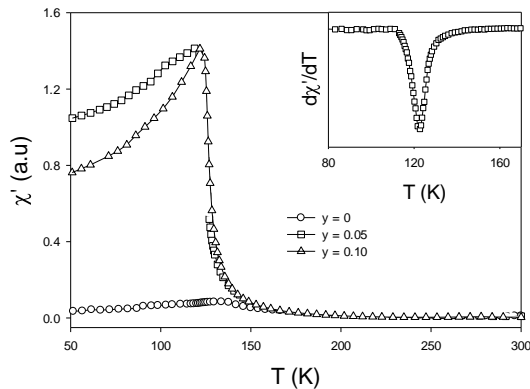
**Fig. 1:** X-ray powder diffraction pattern of $\text{Pr}_{0.75}\text{Na}_{0.25-y}\text{Ag}_y\text{MnO}_3$ ($0 \leq y \leq 0.10$)**Fig. 2:** SEM images with 5kX magnification for $\text{Pr}_{0.75}\text{Na}_{0.25-y}\text{Ag}_y\text{MnO}_3$ samples (a) $y = 0$, (b) $y = 0.05$ and (c) $y = 0.10$

Figure 3 displays the result of the temperature dependence of AC susceptibility (χ') measurement for all samples. The AC susceptibility (χ') data showed the $y = 0$ sample exhibits paramagnetic (PM) to anti-ferromagnetic (AFM) transition at T_N of 129 K. This is most likely related to the existing of CO state arising from the ordering of Mn^{3+} and Mn^{4+} ions in line with a previous suggestion for $\text{Pr}_{0.75}\text{Na}_{0.25}\text{MnO}_3$ [11]. Our results also showed that increasing Ag-doped induced PM to ferromagnetic (FM)-like with T_C around 124 K for $y = 0.05$ sample most likely due to revival of the double exchange (DE) mechanism [12]. However, increasing of Ag-doped up to $y = 0.10$ suppress back the ferromagnetic (FM) to AFM states with T_N around 122 K suggestively due to the

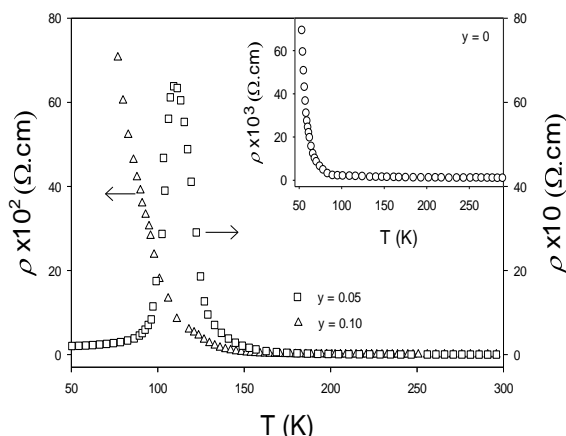
Table 1: MI transition temperature (T_{MI}), Curie temperature (T_C), Neel temperature (T_N), lattice parameters, unit cell volume (V), density (D) and porosity (C) of $\text{Pr}_{0.75}\text{Na}_{0.25-y}\text{Ag}_y\text{MnO}_3$ ($0 \leq y \leq 0.10$)

Samples	T_{MI} (K) ± 0.1	T_C (K) ± 0.1	T_N (K) ± 0.1	Lattice parameter ± 0.001			$V(\text{\AA}^3)$ ± 0.1	$D(\text{g/cm}^3)$ ± 0.01	C (%) ± 0.01
				a (\AA)	b (\AA)	c (\AA)			
$y = 0.0$	-	-	125.0	5.432	7.680	5.451	227.4	6.26	6.31
$y = 0.05$	110.0	123.0	-	5.437	7.697	5.452	228.1	6.41	3.68
$y = 0.10$	-	-	126.0	5.459	7.705	5.455	229.5	6.54	1.01

weakening of DE mechanism. In fact, a similar suggestion was also proposed for $\text{Nd}_{0.75}\text{Na}_{0.25}\text{Mn}_{1-x}\text{Cr}_x\text{O}_3$ [19].

**Fig. 3:** Temperature dependence of AC susceptibility of $\text{Pr}_{0.75}\text{Na}_{0.25-y}\text{Ag}_y\text{MnO}_3$ ($0.0 \leq y \leq 0.10$). Inset is $d\chi'/dT$ vs T for $y = 0.05$

The effect of Ag-doped on electrical resistivity (ρ) measurement of the $y = 0 - 0.10$ samples was shown in Figure 4. It was found that, the $y = 0$ sample (inset Figure 4) showed an insulating behaviour in the temperature range of 50–300 K. Interestingly, metal-insulator (MI) transition was observed at temperature around $T_{MI} \sim 111$ K for $y = 0.05$ sample which can be attributed due to the double exchange (DE) mechanism. In fact, our finding is in line with the previous study [20]. However, no MI transition temperature was observed for $y = 0.10$ sample most likely due to the suppression of DE mechanism as a result of inclining of charge ordering (CO) state [19,21]. In addition, the suppression of the DE mechanism for the sample is also supported by the absence of the Curie temperature T_C as well as existing of Neel temperature T_N in susceptibility measurement.

**Fig. 4:** Temperature dependence of electrical resistivity for $\text{Pr}_{0.75}\text{Na}_{0.25-y}\text{Ag}_y\text{MnO}_3$ ($0.0 \leq y \leq 0.10$)

4. Conclusion

In conclusion, the effect of Ag-doping at Na site of $\text{Pr}_{0.75}\text{Na}_{0.25-y}\text{Ag}_y\text{MnO}_3$ ($0 \leq y \leq 0.10$) on structure and surface

morphological as well as electrical transport and magnetic properties have been investigated. The crystal structure of all samples was found in an orthorhombic structure with space group $Pnma$ where the values of lattice parameter, unit cell volume and density, as well as porosity increase continuously with Ag content, accompany with the improvement of grain boundaries determined from SEM images which can be attributed due to the of difference in ionic radius between Na^+ and Ag^+ ions. On the other hand, AC susceptibility and DC electrical resistivity measurements showed the sample of $y = 0.05$ exhibited ferromagnetic-metallic (FMM) phase suggestively due to the DE mechanism causing the CO state to become weakened. However, an insulating behavior and PM to AFM phase with Neel temperature around $T_N \sim 125$ K and $T_N \sim 126$ K were observed for $y = 0$ and $y = 0.10$ samples respectively.

Acknowledgement

This research was supported by Geran Penyelidikan Pascasiswazah (GPPS) vot U974 from Universiti Tun Hussein Onn Malaysia. The author would like to thank the Ceramics and Amorphous Group, Faculty of Applied Sciences and Technology, Pagoh Higher Education Hub, Universiti Tun Hussein Onn as well as Superconductor Laboratory, Faculty of Applied Sciences, Universiti Teknologi MARA Shah Alam, for the facilities provided.

References

- [1] Sankarajan S, Aravindan S, Yuvakkumar R, Sakthipandi K & Rajendran V (2009), Anomalies of ultrasonic velocities, attenuation and elastic moduli in $\text{Nd}_{1-x}\text{Sr}_x\text{MnO}_3$. *Journal of Magnetism and Magnetic Material* 321, pp. 3611–3620.
- [2] Orlova TS, Laval JY, Monod Ph, Noudev JG & Greshnov AA (2013), Universal effect of Mn-site doping on charge ordering in $\text{La}_{1/3}\text{Ca}_{2/3}\text{MnO}_3$. Universal effect of Mn-site doping on charge ordering in $\text{La}_{1/3}\text{Ca}_{2/3}\text{MnO}_3$. *Journal of Magnetism and Magnetic Material* 342, pp. 120–127.
- [3] Gor'kov LP & Kresin VZ (2004), Mixed-valence manganites: Fundamentals and main properties. *Physics Reports* 400, 149–208.
- [4] Millis AJ, Littlewood PB & Shraiman BI (1995), Double exchange alone does not explain the resistivity of $\text{La}_{1-x}\text{Sr}_x\text{MnO}_3$. *Physic Review Letters* 74, pp. 5144–5147
- [5] Raveau B, Herviu M, Maignan A & Martin C (2001), The route to CMR manganites: what about charge ordering and phase separation? *Journal of Material Chemistry* 11, pp. 29–36.
- [6] Liu Y, Kong H & Zhu CF (2007), Coexistence of charge ordering and ferromagnetism in $\text{Nd}_{0.5}\text{Ca}_{0.5}\text{Mn}_{1-x}\text{Co}_x\text{O}_3$ ($x \leq 0.1$). *Journal of Alloys Compound* 439, pp. 33–36.
- [7] Hejtmánek J, Jiráček Z, Šebek J, Strejček A, Herviu M, & Strejček A (2001), Magnetic phase diagram of the charge ordered manganite $\text{Pr}_{0.8}\text{Na}_{0.2}\text{MnO}_3$. *Apply Physics* 89, pp. 51–54.
- [8] Satoh T, Kikuchi Y, Miyano K, Jira Z, Pollert E & Hejtma J (2002), Irreversible photoinduced insulator-metal transition in the Nd-doped manganite $\text{Pr}_{0.75}\text{Na}_{0.25}\text{MnO}_3$. *Physical Review B* 65, pp. 1–4.
- [9] Phong PT, Khien NV, Dang NV, Manh DH, Hong LV, & Lee II (2015), Effect of Pb substitution on structural and electrical transport of $\text{La}_{0.7}\text{Ca}_{0.3-x}\text{Pb}_x\text{MnO}_3$ ($0 \leq x \leq 0.3$) manganites. *Physica B: Condensed Matter* 466, pp. 44–49.
- [10] Shamsuddin S, Ibrahim ABM & Yahya AK (2013), Effects of Cr substitution and oxygen reduction on elastic anomaly and ultrasonic velocity in charge-ordered $\text{Nd}_{0.5}\text{Ca}_{0.5}\text{Mn}_{1-x}\text{Cr}_x\text{O}_{3-\delta}$ ceramics. *Ceram. Ceramics International* 39, pp. S185–S188

- [11] Rozilah R, Ibrahim N, Mohamed Z, Yahya AK, Khan NA, & Khan MN (2017), Inducement of ferromagnetic-metallic phase in intermediate-doped charge-ordered $\text{Pr}_{0.75}\text{Na}_{0.25}\text{MnO}_3$ manganite by K^+ substitution. *Physical B: Physics of Condensed Matter* 521, pp. 281–294.
- [12] Tarhouni S, Mleiki A, Chaaba I, Khelifa H Ben, Koubaa M, Cheikhrouhou A & Hlil EK (2017), Structural, magnetic and magnetocaloric properties of Ag doped $\text{Pr}_{0.5}\text{Sr}_{0.5-x}\text{Ag}_x\text{MnO}_3$ manganites ($0.0 \leq x \leq 0.4$). *Ceramics International* 43, pp. 133–143.
- [13] Hcini S, Zemni S, Triki A, Rahmouni H & Boudard M (2011), Size mismatch, grain boundary and bandwidth effects on structural, magnetic. *Journal of Alloys and Compound* 509, pp. 1394–1400.
- [14] Zawawi R A, Ibrahim N & Shamsuddin S (2018), Enhancement of double-exchange mechanism in charge-ordered $\text{Pr}_{0.75}\text{Na}_{0.25}\text{MnO}_3$ ceramic by Cr doped at Mn-site. *International Journal Current Science, Engineering and Technology* 1(S1): pp. 101–106.
- [15] AB Mannan NN, Shamsuddin S, Noh MZ & Mohamed Z (2018), Crystalline phase, surface morphology and electrical properties of monovalent doped $\text{Pr}_{0.75}\text{Na}_{0.25}\text{Mn}_{1-x}\text{Co}_x\text{O}_3$. *International Journal Current Science, Engineering and Technology* 1(S1), pp. 220–225.
- [16] Elyana E, Mohamed Z, Kamil SA, Supardan SN, Chen SK, & Yahya AK (2018), Revival of ferromagnetic behavior in charge-ordered $\text{Pr}_{0.75}\text{Na}_{0.25}\text{MnO}_3$ manganite by ruthenium doping at Mn site and its MR effect. *Journal of Solid State Chemistry* 258, pp. 191–200.
- [17] Li Y, Miao J, Sui Y, Lü Z, Qian Z, & Su W (2006), Phase separation, low-field magnetic and transport properties of $\text{Pr}_{0.75}\text{Na}_{0.25}\text{Mn}_{0.9}\text{Fe}_{0.1}\text{O}_3$. *Journal of Magnetism and Magnetic Material* 305, pp. 247–252.
- [18] Khelifa HB, Othmani S, Chaaba I, Tarhouni S, Cheikhrouhou-koubaa W, Koubaa M, Cheikhrouhou A & Hlil EK (2016), Effect of K-doping on the structural, magnetic and magnetocaloric properties of $\text{Pr}_{0.8}\text{Na}_{0.2-x}\text{K}_x\text{MnO}_3$ ($0 \leq x \leq 0.15$) manganites. *Journal of Alloys and Compound* 680, pp. 388–396
- [19] Zhang X & Zhiqing LI (2011), Influence of Cr-doping on the magnetic and electrical transport properties of $\text{Nd}_{0.75}\text{Na}_{0.25}\text{MnO}_3$. *Journal of Rare Earths* 29, pp. 230–234.
- [20] Shamsuddin S, Ibrahim ABM, & Yahya AK (2013), Effects of Cr substitution and oxygen reduction on elastic anomaly and ultrasonic velocity in charge-ordered $\text{Nd}_{0.5}\text{Ca}_{0.5}\text{Mn}_{1-x}\text{Cr}_x\text{O}_{3-\delta}$ ceramics. *Ceramics International* 39, pp. S185–S188.
- [21] Arifin M, Ibrahim N, Mohamed Z, Yahya AK, Khan NA & Khan MN (2018), Revival of Metal-Insulator and Ferromagnetic-Paramagnetic Transitions by Ni Substitution at Mn Site in Charge-Ordered Monovalent Doped $\text{Nd}_{0.75}\text{Na}_{0.25}\text{MnO}_3$ Manganites. *Journal of Superconductivity and Novel Magnetism*, pp. 1–18. <https://doi.org/10.1007/s10948-017-4521-7>